Supporting Information

Hollow core-shell MnO_2-NT/NiMn-LDH/NiS electrode for enhanced supercapacitor performance

Jiahong Zheng[*]*, Yuhan Wang, Jingyun Yang*

Materials

All chemicals were used as analytical-reagent grade without further purification: Manganese (II) Sulfate Monohydrate ($MnSO_4 \cdot H_2O$, ≥99%, Sinopharm Chemical Reagent Co., Ltd), Potassium Chlorate ($KClO_3$, ≥98%, Tianjin Damao), Potassium Acetate (CH_3COOK, ≥99%, Tianjin Damao), Tannic Acid (TA) ($C_{76}H_{52}O_{46}$, AR, Tianjin Damao), Poly Dimethyl Diallyl Ammonium Chloride (PDDA) ($(C_8H_{16}NCl)_n$, ≥20%, XILONG SCIENTIFIC), Hexamethylenetetramine (HMT, ≥99.5%, CHRON CHEMICALS), Nickel (II) Chloride Hexahydrate ($NiCl_2 \cdot 6H_2O$, ≥99.9%, Tianjin Damao), Manganese (II) Chloride Tetrahydrate ($MnCl_2 \cdot 4H_2O$, ≥99%, XILONG SCIENTIFIC) and Thioacetamide (TAA, ≥99%, Aladdin).

Characterization

To determine the crystal structure of the sample, we used an instrument called X-ray diffractometer (XRD, Bruker D8AA25). This instrument can infer the crystal structure of a sample by measuring its X-ray diffraction pattern. we used a scanning electron microscope (SEM, Hitachi S-4800, Japan) to observe the microstructure of the

Address correspondence to E-mail: jhzheng@chd.edu.cn (J.H. Zheng)
Tel: 86-029-82337340 Fax: 86-029-82337340

sample. Meanwhile, we also utilized transmission electron microscopy (TEM, Tecnai F30G2) to further analyze the internal morphology of the samples. we also used X-ray photoelectron spectroscopy (XPS, ESCALAB Xi+) to analyze the molecular structure, elemental valence states, and chemical bonding information of the samples. The porous nature, pore size distribution and surface area of the samples were examined by nitrogen adsorption-desorption isotherm (BET) and Barrett-Joyner-Halenda (BJH) approaches in an automated gas sorption analyzer (ASAP2020HD88).

Electrochemical measurements and necessary equations

The electrochemical performance of the samples in both three-electrode and two-electrode systems were evaluated using an electrochemical workstation (CHI660E, Shanghai Chenhua). In three electrode system, Pt is the counter electrode and saturated calomel is used as the reference electrode. In addition, MnO_2-NT/NiMn-LDH/NiS and activated carbon (AC) as positive and negative electrodes to assemble the ASC, respectively. Calculate specific capacitance (C), power density (E), and energy density (P) of electrode materials based on equations (1), (2), and (3), respectively.

$$C = \frac{I \times \Delta t}{M \times \Delta V} \tag{S1}$$

In the formula: C is the specific capacitance, unit: $F \cdot g^{-1}$; I is the discharge current, in A; Δt is the discharge time, in seconds; M is the mass of the active substance, in grams; ΔV is the potential range of discharge, measured in V.

$$E = \frac{C \times \Delta V^2}{7.2} \tag{S2}$$

$$P = \frac{E \times 3600}{\Delta t} \tag{S3}$$

Supplementary Figures

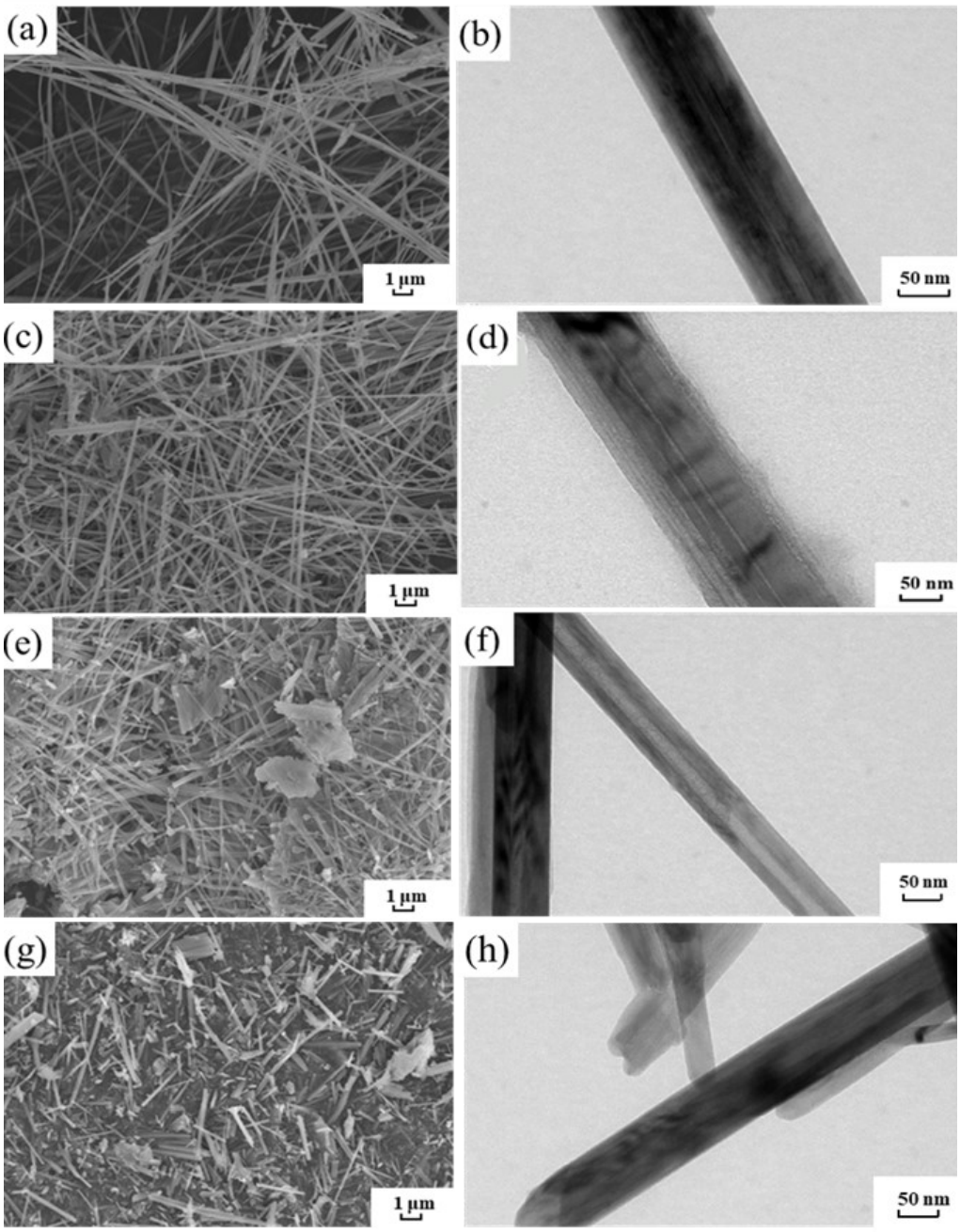

Figure S 1. SEM and TEM images of (a-b) 0 mg·mL^{-1}, (c-d) 1 mg·mL^{-1}, (e-f) 5 mg·mL^{-1}, (g-h) 10 mg·mL^{-1}.

SEM and TEM images of MnO_2 at different TA concentrations with reaction temperature and reaction time of 30 °C and 10 min. Fig. S1a and b† show the SEM and TEM images of MnO_2 when TA concentration is 0, respectively. It can be seen from

the images that the morphology of MnO_2 is nanowires with a length of about 150 μm and a diameter of about 80 nm, and the dispersion is good. When the concentration of TA increased to 1 mg·mL^{-1}, the SEM and TEM images of MnO_2 were shown in Fig. S1c and d†. The length and diameter of MnO_2 barely changed, but a large number of holes appeared. When the concentration of TA was further increased to 5 mg·mL^{-1} (Fig. S1e-f†), the morphology of MnO_2 became nanotube, the length remained unchanged, the diameter decreased to about 50 nm, and the tube wall thickness was about 20 nm. When the concentration of TA was further increased to 10 mg·mL^{-1}, the sample showed serious fracture and agglomeration, with a length of about 5-20 μm, as shown in Fig. S1g and h†. This may be due to the stricter etching of MnO_2-NW by too high concentration of tannic acid, resulting in fracture and gradual agglomeration during continuous stirring. Combined with the subsequent electrochemical performance analysis, the optimal concentration of TA was 5 mg·mL^{-1}.

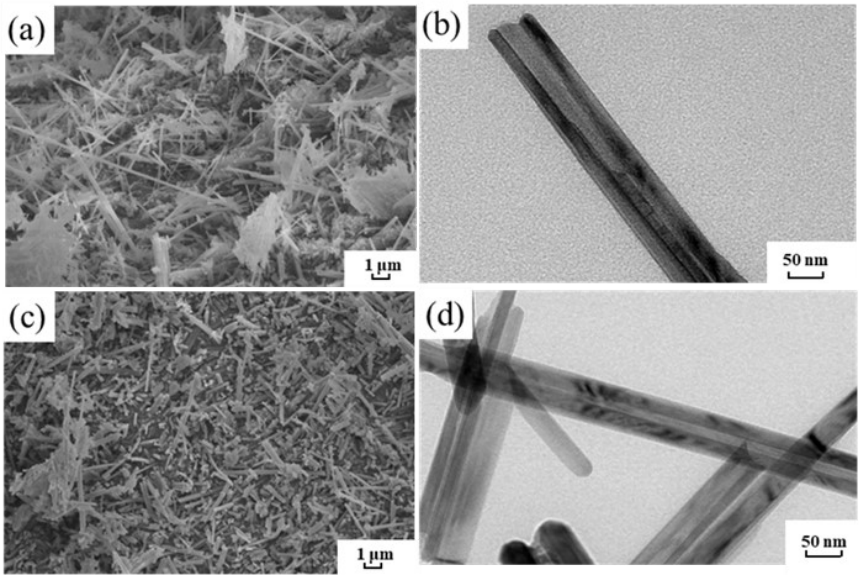

Figure S 2. SEM and TEM images of (a-b) 60 min, (c-d) 120 min.

When the concentration of TA was 5 mg·mL^{-1}, the effect of etching time on the

morphology of MnO_2 was further studied. When the etching time was increased to 60 min and 120 min, the SEM and TEM images of MnO_2 were shown in Fig. S2†. Fig. S2a and b† are SEM and TEM images of MnO_2 when the etching time is 60 min. When the reaction time was increased to 60 min, the sample size was almost unchanged, while the pore size of the nanotubes increased to 40 nm. It shows that with the extension of time, tannic acid will further etch MnO_2-NW. When the time was further extended to 120 min (S2c and d†), the pore size of the nanotubes did not change, and the sample showed a serious fracture phenomenon, and the length was reduced to about 10 μm. Combined with subsequent electrochemical performance analysis, the optimal reaction

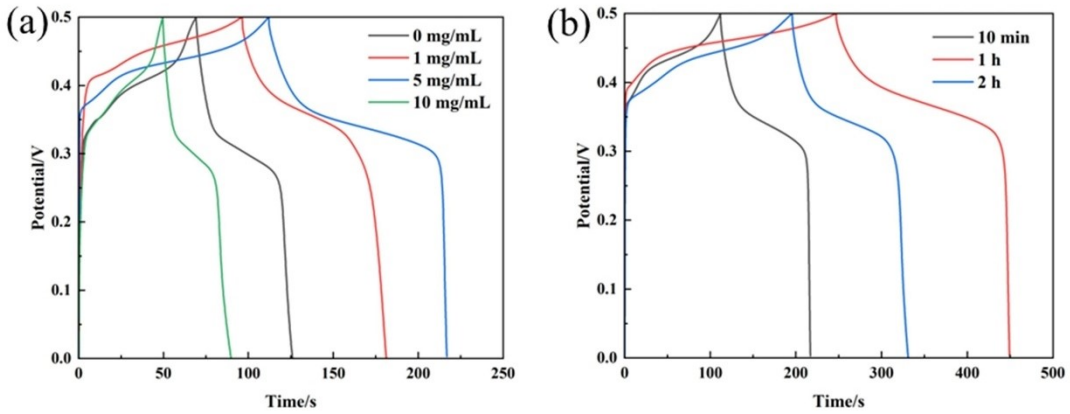

Figure S 3. GCD curves of the different samples at 1 $A \cdot g^{-1}$.

time was 60 min.

The effects of TA concentration and different reaction times on the electrochemical properties were investigated, and the results are shown in Fig. S4†. First, the reaction temperature and reaction time were selected to be 30 ℃ and 10 min, respectively, and the GCD curves of the samples containing different TA additions at a current density of 1 $A \cdot g^{-1}$ are shown in Fig. S4a†. The specific capacitance of the

samples increased and then decreased with the increase of TA concentration. When the TA concentration was 5 $mg \cdot mL^{-1}$, the samples had a maximum specific capacitance of 209.6 $F \cdot g^{-1}$. Fig. S4b† shows the GCD curves of the samples obtained at 1 $A \cdot g^{-1}$ with different reaction times (10 min, 1 h, 2 h) under the conditions of TA concentration of 5 $mg \cdot mL^{-1}$ and reaction temperature of 30 ℃, and the specific capacitances of the three groups of samples were calculated to be 209.6 $F \cdot g^{-1}$, respectively, 404.0 $F \cdot g^{-1}$, and 270.5 $F \cdot g^{-1}$, so the optimal reaction time was 1 h. Combined with the analysis of the above experimental results, the optimal experimental conditions were TA concentration of 5 $mg \cdot mL^{-1}$ and reaction time of 1 h.

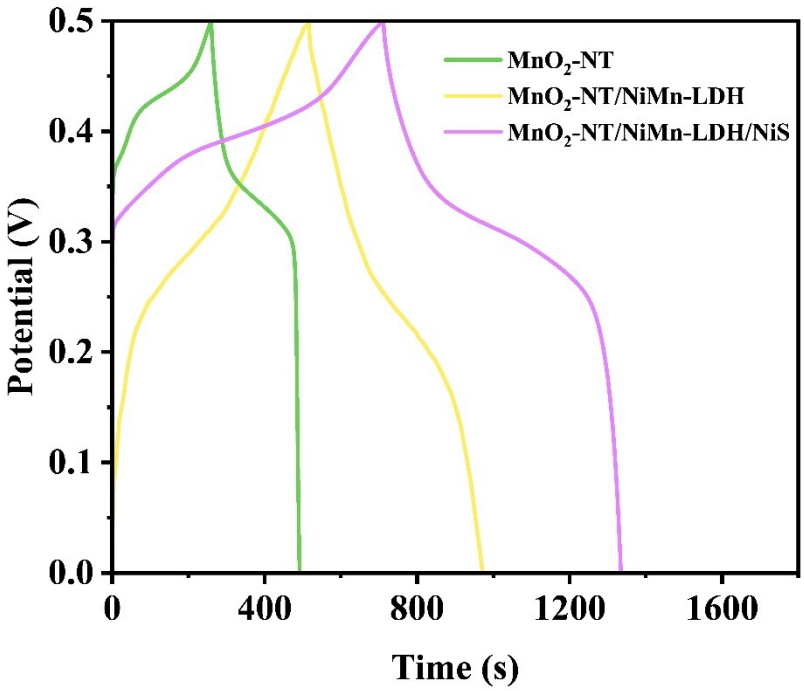

Figure S 4. Comparison of GCD curves of the different samples at 1 $A \cdot g^{-1}$

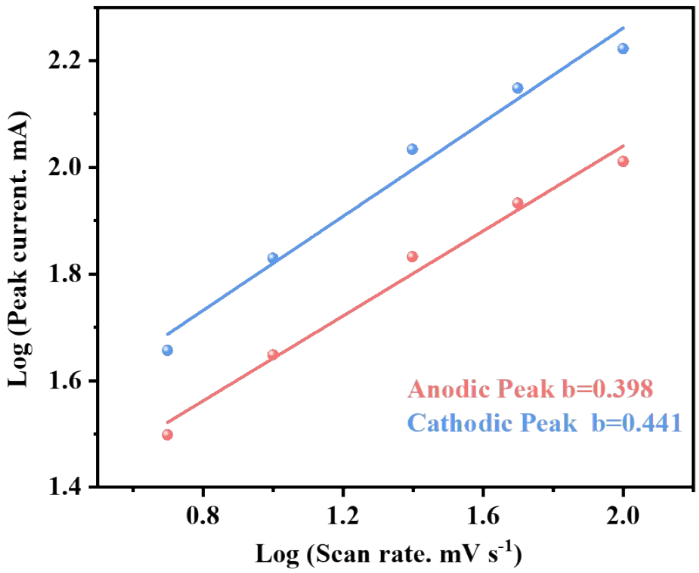

Figure S 5. Logarithmic diagram of peak current versus scan rate for MnO_2-NT/NiMn-LDH/NiS.

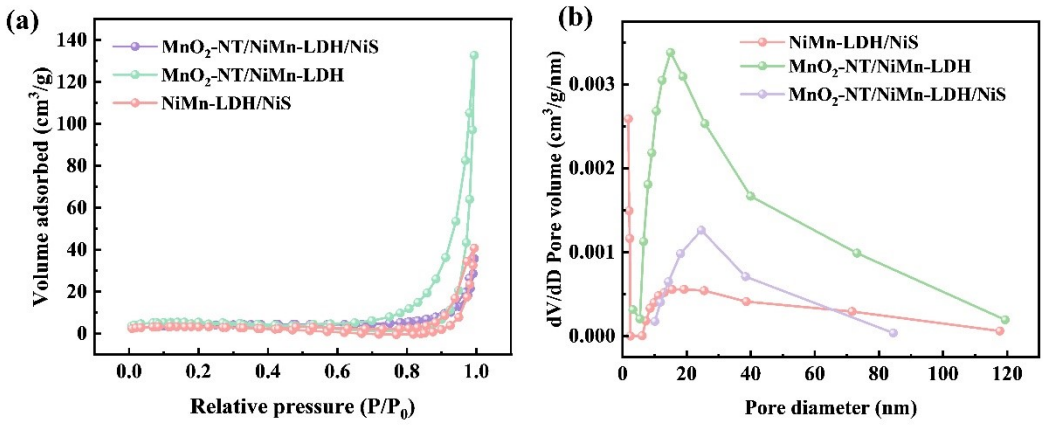

Figure S6. (a) Nitrogen adsorption/desorption isotherms and (b) pore size distributions of different samples.